Wadi Alshatti University Journal of Pure and Applied Sciences

مجلة جامعة وادي الشاطئ للعلوم البحتة والتطبيقية

Volume 4, No. 1, January-June 2026 Online ISSN: 3006-0877 المجلد 4، الاصدار 1، يناير- يونيو 2026

RESEARCH ARTICLE FLUID MECHANICS

Numerical Simulation of 2D Axisymmetric Flow Within Pressure swirl atomizer using InterFoam

Abdallah Salem[1*], Abulhafiz Ahmed Aqila[1], Mohammed Ibrahim Hamdan[2]

[1]Mechancal & Renewable energy Eng. Dept., Engg, Faculty, Wadi Alshatti University, Brack, Libya
[2] Mechanical Engineering Department, Khawarizmi University Technical College, Amman, Jordan

ARTICLE HISTORY
Received 23 November 2025
Revised 19 December 2025
Accepted 22 December 2025
Online 25 December 2025

KEYWORDS
Pressure swirl atomizer;
2D axisymmetric simplex atomizer;
InterFoam;
Volume of fluid.

ABSTRACT

This study evaluates the open-source CFD solver InterFoam for simulating multiphase flow in a 2D axisymmetric pressure-swirl atomizer using water and air. Motivated by the computational and experimental constraints of 3D studies, the research investigates two atomizer dimensions under a laminar flow assumption. The Volume of Fluid (VOF) method and Continuum Surface Force (CSF) model are employed for interface tracking and surface tension. Qualitatively, the solver accurately captures key flow features, including air-core formation, swirling sheet emanation, and characteristic low-pressure distributions. Quantitatively, interFoam shows excellent agreement with experimental data for Case 1, with average swirling velocity errors of 6.11% at the inlet and 7.18% at the exit. However, Case 2 resulted in significant errors (49.05% and 14.43%) because the laminar assumption is invalid at the high Reynolds number (Re = 74,246) present. This highlights the necessity of turbulence modeling for high-Re pressure-swirl flows. Finally, the solver's performance in predicting the flow number, discharge coefficient, and spray cone angle outperformed literature findings based on inviscid analysis and maximum flow theory. The results suggest that accurate representation of swirling velocity profiles, alongside the swirl number, serves as a critical indicator for when turbulence models must be adopted.

محاكاة ثنائية البعد ومثماتلة لرشاش ضغط دوامي بإستخدام برنامج الانترفوم

عبدالله سالم[1]*، عبدالحفيظ أحمد عقيلة [1]، محمد ابراهيم حمدان[2]

الملخص

تُقيّم هذه الدراسة أداء برنامج **interFoam** في محاكاة التدفق متعدد الأطوار لرشاش ضغط دوامي ثنائي الأبعاد، باستخدام الماء والهواء. الدافع وراء الدراسة هو صعوبة تنفيذ محاكاة ثلاثية الأبعاد أو تجارب معملية لنقص الموارد. تناولت الدراسة بُعدين مختلفين للمدخل بافتراض جريان انسيا بي، واستخدام طريقة (VOF) حجم المائع لتتبع الواجهة ونموذج قوى السطح االمستمرة (CSF) للتوتر السطحي.أظهر البرنامج قدرة قوية على رصد ملامح التدفق نوعياً، بما في ذلك تشكل النواة الهوائية وانبثاق الطبقة الدوارة وتوزيع الضغط المنخفض. كمياً، حقق **interFoam**توافقاً ممتازاً في الحالة الأولى بمتوسط خطأ 6.11% و7.18% عند المدخل والمخرج. ومع ذلك، فشل في التنبؤ بملفات السرعة في الحالة الثانية بأخطاء بلغت 49.05% و14.43%، نتيجة افتراض الجريان الطباقي عند رقم رينولدز مرتفع جداً.(Re = 74,246) .تشير هذه النتائج لضرورة اعتماد نماذج الاضطراب (turbulence models) للسرعات العالية في هذا النوع من الرشاشات. أخيراً، أثبت **interFoam** كفاءة أعلى في التنبؤ بخصائص التدفق في الرشاش (رقم التدفق، معامل التصريف، وزاوية الرش) مقارنة بالدراسات النظرية المعتمدة على التحليل غير اللزج ونظرية التدفق الأقصى. كما أكدت الدراسة أن التمثيل الدقيق لملفات السرعة، إلى جانب رقم الدوران، يعد مؤشراً حاسماً للحاجة لاستخدام نماذج الاضطراب.

الكلمات المفتاحية
رشاش الضغط الدوامي
رشاش متماثل وتنائي البعد
الانترفوم
حجم المائع

Introduction

A liquid sheet emanating from a pressure-swirl atomizer has the most significant surface-to-volume ratio among atomizers, including circular, planar, and cylindrical. This feature makes the simplex atomizer the best choice for a wide range of applications, including aircraft and marine engines, spray coating systems, chemical processing units, and desalination plants. The simplex atomizer, which is the simplest configuration of a pressure-swirl atomizer, consists of a cylindrical chamber followed by a conical chamber and an exit orifice. The liquid is injected into the conical chamber using one or more tangential ports. Once the fluid enters the conical chamber, it experiences a high inertial force relative to its surface tension. As a result of this high angular momentum inside the cylindrical chamber, a gas core starts to form inside the chamber. Moreover, the high centrifugal

*Corresponding author
https://doi.org/10.63318/waujpasv4i1_03

force acting on the liquid inside the conical chamber causes the exiting liquid sheet to assume a hollow-cone shape. The conical sheet emanating from the atomizer orifice is subject to strong aerodynamic forces, leading to instability of the sheet surface. Downstream, the sheet begins to disintegrate into ligaments, which is known as primary atomization. Further downstream, the formed ligaments disintegrate into smaller droplets, a process known as secondary atomization. Given its wide range of applications, many studies have examined the internal and external characteristics of the pressure swirl atomizer (PSA). The internal characteristics of PSA include gas-core stability and formation, as well as the boundary-layer thickness. On the other hand, the external characteristics include the sheet thickness, breakup length, spray cone angle, and discharge coefficient [1].

The investigation of PSA flow characteristics can be conducted either experimentally or numerically. The experimental investigation of flow within the pressure-swirl atomizer can be costly and challenging because many critical physical phenomena occur in small spatial regions at extremely high speeds, which require high-resolution and high-speed measurement equipment [2]. On the other hand, numerical simulation is an alternative technique for studying the atomizer's flow characteristics. Yet, achieving high fidelity in 3D numerical simulation is extremely expensive in terms of computational cost [3]. Moreover, the complexity of the flow field in which two incompressible phases coexist is not intuitive. The discontinuity of properties across the phase interface, along with the need for an accurate representation of local curvature and surface tension, requires a large number of computational cells. For example, (Lei et al., (2019)), conducted 3D numerical simulations of flow in a pressure-swirl atomizer to investigate the velocity distribution at the atomizer exit. In their study, 5 million grids were used in the simulation. They managed to visualize the breakup mode of the conical sheet in high resolution. (Julio Ronceros et al., 2024) They also conducted a 3D numerical simulation of a pressure-swirl atomizer to compare it with their theoretical model of PSA flow. In their simulation, 3.5 million computational cells were used. Although the results from their theoretical model match pretty well with those from their numerical simulation, the conical sheet emanating from the atomizer is highly diffusive.

Taking advantage of the symmetry of the atomizer configuration, (Milan Maly et al., (2019)), reduced the total computational cells by one-fourth of the total mesh using periodic boundary conditions. They achieve a sharp interface with a good representation of the velocity fields inside the atomizer.

Many researchers have adopted reducing the 3D configuration to a 2D axisymmetric configuration due to the high computational cost of the 3D case. For example, (Nouri Borujerdi et al., (2012)), implemented a 2D axisymmetric mesh to investigate laminar and turbulent flow within the pressure-swirl atomizer. In their study, the number of computational cells used in the simulation was significantly reduced (to 150,000 cells). Moreover, they visualized the flow within the atomizer, with vortices in the conical chamber well captured.

In another study, (Onur Baran et al., (2019)), conducted an experimental investigation and numerical simulation of a coaxial pressure-swirl atomizer. They used 2D and 3D computational domains. Although the number of computational cells used was not reported, the models achieved comparable results for the mean swirl and axial velocity profiles, indicating the validity of the 2D axisymmetric model.

Although reducing the 3D pressure-swirl atomizer configuration to a 2D axisymmetric configuration can significantly reduce computational expense, numerically simulating such a flow remains challenging, primarily due to the complex interactions between the two phases. Accurately representing the interface requires a Eulerian method, such as the Volume of Fluid (VOF) approach (Hirt and Nichols, 1981). However, discontinuities in the VOF fraction can lead to numerical diffusion unless specialized interface reconstruction schemes are employed. Furthermore, accurate computation of the surface tension force is crucial for atomization (Brackbill et al., 1992). .

Over the last decade, the interFoam solver in the open-source CFD software OpenFOAM has gained significant popularity. It utilizes an algebraic VOF advection algorithm that offers a good balance between computational cost and interface resolution. However, its effectiveness has been assessed; for instance, Deshpande et al. (2012) found that interFoam performs well in inertia-dominated flows but shows limitations in accurately modeling surface-tension-dominated regimes. Recent studies have demonstrated the use of interFoam and its coupled variants for PSAs, including large-scale 3D simulations (D. Fernnando et al., 2021) and enhanced 2D axisymmetric models (A. Salem., 2023). More advanced study by (Austin Han., 2025)) used the volume of fluid and large eddy simulation to investigate the near-nozzle characteristics of the fuel emanating from the pressure-swirl atomizer. Their study matched the experimental results in calculating the breakup length, spray cone angle, and liquid film thickness. Another study conducted by (Ertunc et al., 2025) used 2D and 3D numerical simulations of liquid in a pressure-swirl atomizer. Their studies concluded that Golter vortices in the liquid sheet negatively affect the quality of sheet atomization.

Despite these advancements, a comprehensive and accessible validation of the standard interFoam solver for simulating the key performance characteristics of a 2D axisymmetric PSA against experimental data is still needed.

The primary objective of the present study is thus to numerically investigate the internal flow characteristics of a well-documented pressure-swirl atomizer using the standard interFoam solver in OpenFOAM. This work uses a 2D axisymmetric domain to improve computational efficiency. It focuses on validating the numerical model's ability to accurately predict the discharge coefficient C_d, flow number F_N, and spray cone angle θ°. Furthermore, the tangential velocity (angular velocity responsible for angular momentum and the formation of gas core) at different locations will be investigated and compared with results obtained from experiment conducted by Zhanhua Ma [14].

Numerical Setup

In this section, the solver setup will be addressed. As mentioned earlier, interFoam uses the volume-of-fluid method to capture the interface. The solver adopted an algebraic approach to advect the phase interface [22]. This approach gained popularity due to its ability to reduce computational cost and conserve mass compared with approaches that reconstruct the geometrical interface. To maintain numerical stability and ensure the boundedness of the phase fraction field, the advection of the volume fraction is solved using the MULES (Multidimensional Universal Limiter with Explicit Solution) algorithm with temporal sub-cycling [11]. Furthermore, the surface tension force that

drives the atomization of the liquid sheet is modeled using the continuum surface model [10].
The schematic of the atomizer to be numerically simulated is shown in Figure 1.

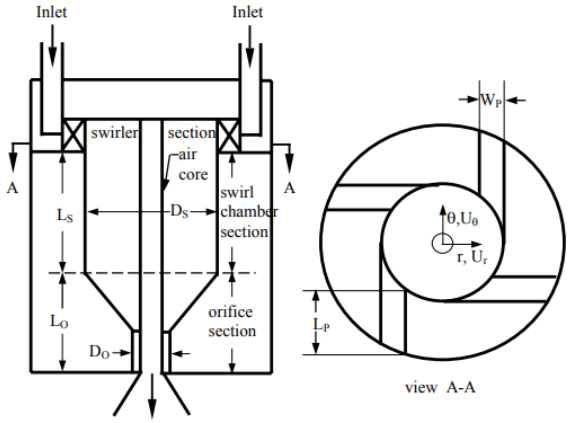

Fig. 1: Schematic of the Pressure Swirl Atomizer [14]

In our study, two different configurations of the atomizer are considered, as shown in Table (1). The two phases used in the simulations are water and air, respectively.

Table 1: The dimensions of the two different configurations considered in the study

Case	A_p mm^2	L_s mm	L_o mm	D_s mm	D_o mm
1	406	89	42	76	21
2	203	89	42	76	21

Governing Equations
For incompressible, isothermal, nonreacting, and immiscible of two-phase flow, the flow is governed by the continuity and momentum equation as flows [11]:

$$\nabla . U = 0 \tag{1}$$

$$\frac{\partial \rho U}{\partial t} + \nabla . (\rho UU) = -\nabla p_d - \nabla \rho \vec{g} . \vec{x} + \nabla . (\mu \nabla U) + (\nabla U) . \nabla \mu + \sigma k \nabla \gamma \tag{2}$$

Where U is the velocity field, p_d is the dynamic pressure, ρ is the density, $\vec{x}$ is the vector position, μ is dynamic viscosity, σ is the surface tension coefficient, γ is the volume fraction field, and k is the local curvature of the interface.
The interface in interFoam is updated using the advection equation of the volume fraction as follows [11]:

$$\frac{\partial \gamma}{\partial t} + \nabla . (U\gamma) + \nabla . [U_r \gamma (1-\gamma)] = 0 \tag{3}$$

Where U_r is the relative velocity of the phase interface, the third term in Eq.3 represents the counter flux which compresses the diffusive interface into a sharper one. The relative velocity can be calculated as follows [11]:

$$U_r = n_f \, min\left(C_\alpha \left| \frac{\varphi}{S_f} \right|, max\left(\frac{|\varphi|}{|S_f|} \right) \right) \tag{4}$$

Where, n_f is cell normal flux, $\left|\frac{\varphi}{S_f}\right|$ is the magnitude of the velocity, φ is the cell face volume flux, and S_f is the cell face surface area, C_α *is* a user-specified compression factor which can vary from 0 to 1.
The viscosity and the density in each computational cell are calculated as follows [11]:

$$\mu = \gamma\mu + (1-\gamma)\mu \tag{5}$$

$$\rho = \gamma\rho + (1-\gamma)\rho \tag{6}$$

The Physical Model of 2D Axisymmetric
The physical domain of the 2D axisymmetric pressure swirl atomizer is shown in Figure (2).

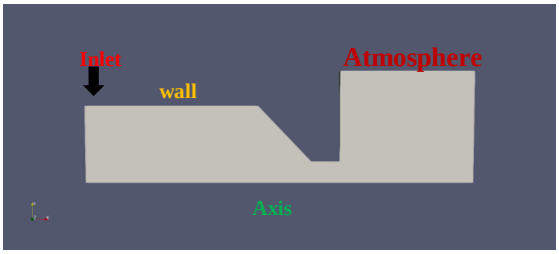

Fig. 2: The 2D physical Model of pressure-swirl atomizer
The angle of symmetry was chosen to be less than 5° (particularly4°),which is expected to reduce the computational cost by factor of $\frac{360^\circ}{4^\circ} = 90$

To achieve the equivalent flow field of the 3D case in 2D axisymmetric geometry, the angular momentum, kinetic energy, and fluid injection thickness must be matched. Thus, the axial velocity w_i is obtained by matching the angular momentum as follows [15]:

$$w_i = \frac{Q}{A_p}\left[\frac{D_s - D_o}{D_s}\right] \tag{7}$$

Where Q is the total volume flow rate, D_s as shown in Figure (1) is the chamber diameter, D_o is the orifice diameter, and A_p is the port cross-sectional area.
The radial velocity v_i is obtained by matching the kinetic energy as follows:

$$v_i = \sqrt{\left(\frac{Q}{A_p}\right)^2 - w_i^2} \tag{8}$$

To conserve the equivalent volume flow rate, the thickness t at which the fluid flows is given by:

$$t = \frac{Q}{\pi D_s w_i} \tag{9}$$

Flow condition
In our study, we chose water and air as the two phases in the atomizer to ensure the simulation is compatible with the experiment conducted by Zhanhua Ma [14]. Moreover, we applied two different flow conditions for each case, as shown in Table (2). Furthermore, we inserted the Reynolds and Weber numbers for each case in the table, which can be calculated as follows, respectively:

$$Re = \frac{v_{in}\, \rho\, L}{\mu} \tag{10}$$

$$We = \frac{\rho\, v^2 L}{\sigma} \tag{11}$$

Where, v_{in} is the velocity inlet to the port of the atomizer, L

is the hydraulic length, and σ is the surface tension coefficient.

Table 2: flow rates, Weber, and Reynolds Numbers for the two different cases

Case	Flow rate; Gallon/minutes	Reynolds number	Weber number
1	10	35253	760.38
	20	70528	3043.51
2	7.5	37294	1207.35
	15	74246	4827.6

The high Reynolds number in all cases justifies the use of interFoam to model the high-inertial flow inside the atomizer. However, we consider the laminar-flow case in our numerical simulations, since the exact Reynolds number is not well-defined; some studies use the inlet-port hydraulic diameter as the characteristic length, while others use the swirl-chamber diameter [16].In their study, Xie et al. [15] applied both the laminar and Reynolds stress model (RSM) to their numerical simulation of the 2D axisymmetric pressure-swirl atomizer at a high Reynolds number of 21196. Both models captured the atomizer's flow characteristics, which justifies the implementation of laminar flow in the simulations. Thus, the simulation in this study will be limited to laminar flow only.

Computational Domain

The computational domain was created using BlockMesh utility in OpenFoam. The utility generated a structured hexahedral mesh. The total number of computational cells in the study was chosen to be 127100 cells, as shown in Figure (3).

To ensure that the number of computational cells is sufficient, we test grid sensitivity by summing the average volume fraction within the computational domain (where x <= 0.131, the region inside the swirl chamber and orifice, aligned with the axial flow). In this context, we used three different numbers of grids, particularly 55800, 127100, and 254200 cells. We test the grid sensitivity by adding the following piece of code at the end of the interFoam source code (interFoam.C) as follows:

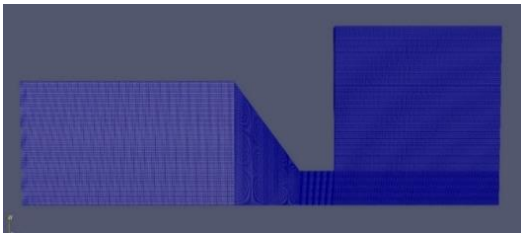

Fig. 3: The computational domain of the 2D axisymmetric atomizer

```
scalar total = 0.0;
scalar n = 0.0;
forAll (mesh.C(), celli)
{
   if (mesh.C()[celli].component(0) <= 0.131)
{
    ; total += alpha1[celli]
n++;
  }
}
scalar average = total / n;
Info << "\nThe average value of alpha1 inside the atomizer is: " <<
average << endl;
Info << "End\n" << endl;
```

The average volume fraction in the computational domain for the three cell counts is shown in Table (3).

Table 3: The average volume fraction of three different numbers of grids

The total number of computational cells	The average volume fraction inside the atomizer
55800	0.7355993
127100	0.7428154
254200	0.7419312

Thus, the number of computational cells of 127100 is fairly sufficient.

The flow chart of the numerical algorithm of the interFoam solver is shown in Figure (4).

The boundary condition

In the simulations, we implement the following boundary conditions for the pressure, velocity, and volume fraction fields, as shown in Table (4)

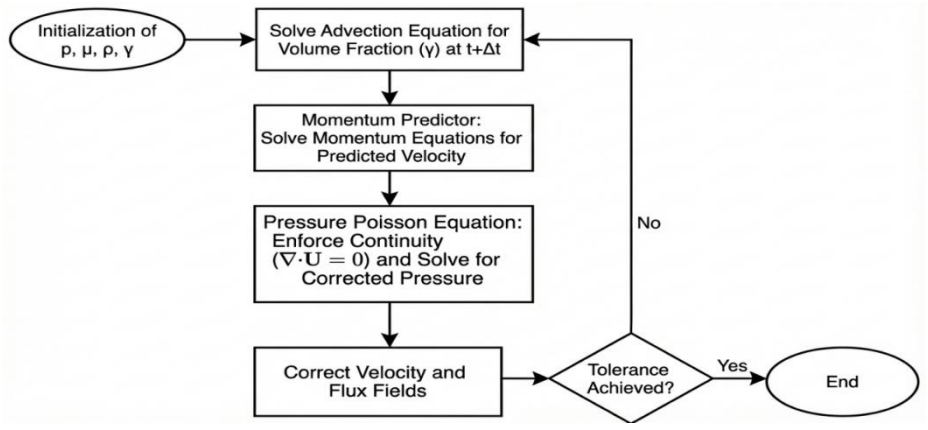

Fig. 4: The numerical algorithm of interFoam solver

Table 4: The boundary condition used in the simulations

Field	Inlet	walls	Atmosphere
Velocity	Fixed Value	No slip	Pressure inlet outlet
pressure	Fixed Flux pressure	Zero Gradient	Total pressure
Volume fraction	Fixed value	Zero Gradient	InletOutlet

Results and discussions

Visualization of the volume fraction in the pressure swirl atomizer

As mentioned above, the results of the numerical simulation will be compared with those of the experiment conducted by Zhanhua Ma in 2002 [4]. The experimental results of the atomizer are shown in Figure (5).

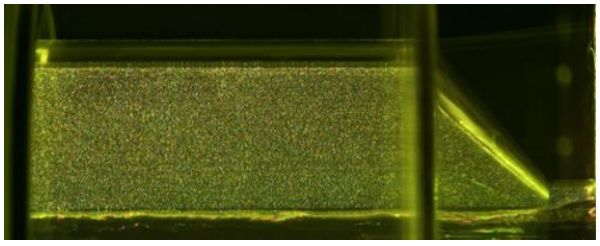

Fig. 5: The experimental result of PSA [14]

Figures (6) and (7) show the volume fraction distribution in the pressure-swirl atomizer obtained by numerical simulation for the first case, with volume flow rates of 10 and 20 gallons per minute, respectively.

Figures (8) and (9) show the volume fraction distribution in the pressure-swirl atomizer obtained by numerical simulation for the second case, with volume flow rates of 7.5 and 15 gallons per minute, respectively.

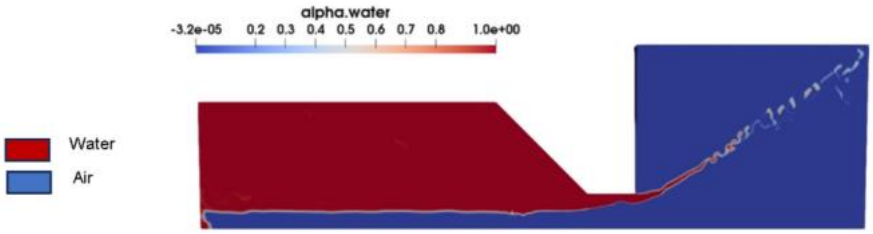

Fig. 6: The volume fraction distribution for 10 gallons/min

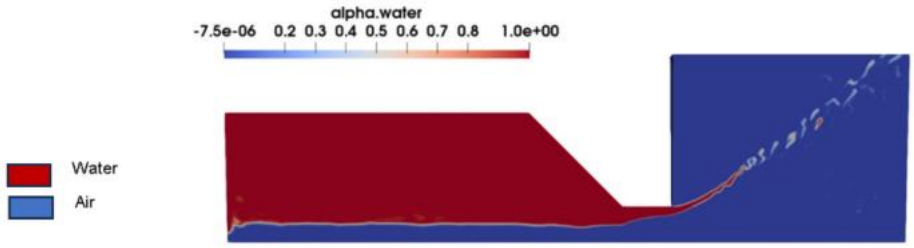

Fig. 7: The volume fraction distribution for 20 gallons/min

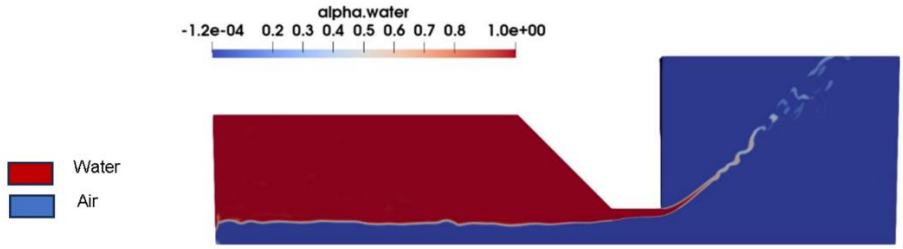

Fig. 8: The volume fraction distribution for 7.5 gallons/min

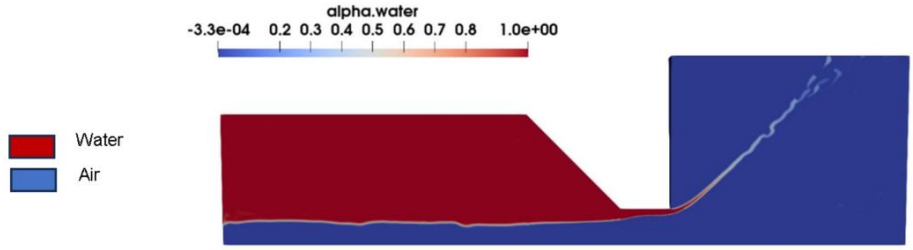

Fig. 9: The volume fraction distribution for 15 gallons/minute

From the numerical simulation results, we observed that the interFoam solver effectively captures the phase interface sharply, particularly in the atomizer, where inertial forces are exceptionally high, leading to a stable air core. Furthermore, compared with the experiment, the radius of the air core obtained by simulations for case one, as shown in figures 6 and 7, is relatively consistent with that shown in figure 4. However, the swirling sheet emanating from the atomizer is highly diffusive because the surface tension force is weakly represented.

Pressure distribution

Figures (10) and (11) show the dynamic pressure distributions obtained from numerical simulations of the first case (volume flow rate of 20 gallons/minute) and the second case (volume flow rate of 15 gallons/minute). It must be noted that p_rgh in the Figures is the dynamic pressure measured in Pascal.

From the numerical simulation results, we observed that low-

pressure regions form within the atomizer where the air core is generated. The radial pressure gradient increases and smears out near the phase interface.

Swirling velocity distribution

Figures (12) and (13) show the angular velocity distribution obtained by numerical simulation for the first case, where the volume fraction is 20 gallons per minute, and the second case, where the volume flow rate is 15 gallons per minute.

From the numerical simulations, the swirling velocity (Tangential velocity) is at its maximum near the air core (in the water phase) with a maximum value of 7.2 m/s, and a negative velocity with a value of -0.24 m/s was observed, which indicates the reverse flow of the air phase from outside (atmosphere) to the inside of the atomizer. Furthermore, the existing sheet has the maximum swirling sheet. The formation of vortices inside and outside the atomizer can also be observed.

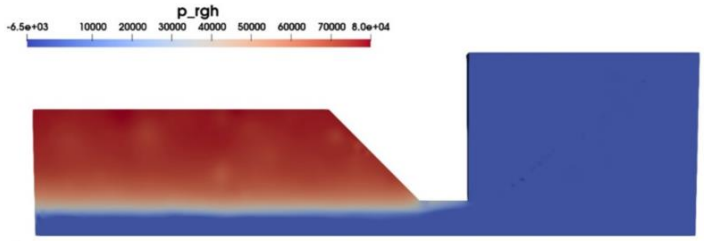

Fig. 10: The pressure distribution in the atomize for case 1 with 20 gallons/minute

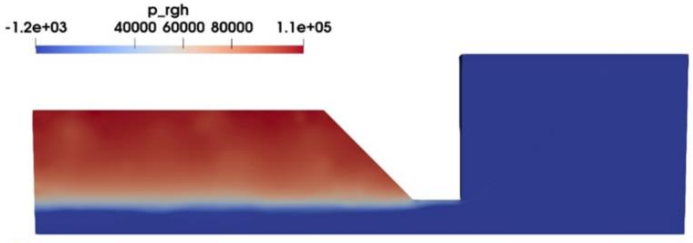

Fig. 11: The pressure distribution in the atomize for case 1 with 20 gallons/minute

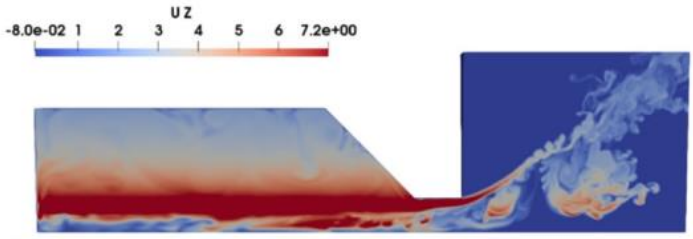

Fig. 12: The distribution of the swirling velocity for case 1 with 20 gallons/min

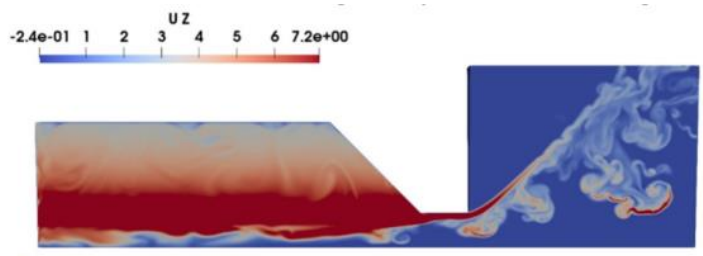

Fig. 13: The distribution of the swirling velocity for the second case with 15 gallons/minute

3.4 Angular Velocity at the inlet and outlet

To better assess interFoam's performance, the numerical simulation results for angular velocity at the inlet and outlet along the radial distance of the atomizer are compared with experimental results [14].

Figures (14) and (15) show the angular velocity profiles along the radial distance for case 1 with volume flow rates of 20 gallons/minute at the inlet and outlet, respectively.

It can be observed that the interFoam for the 2D axisymmetric pressure-swirl atomizer model reasonably predicts the swirling velocity, comparing well with the experimental results, particularly close to the axis of symmetry. However, as we approach the radius of the swirling chamber, r sub s, the numerical results begin to deviate from the experimental results.

Figures (16) and (17) show the angular velocity profiles along the radial distance for case 2 with volume flow rates of 7.5 gallons/minute and 15 gallons/minute at the inlet and outlet, respectively.

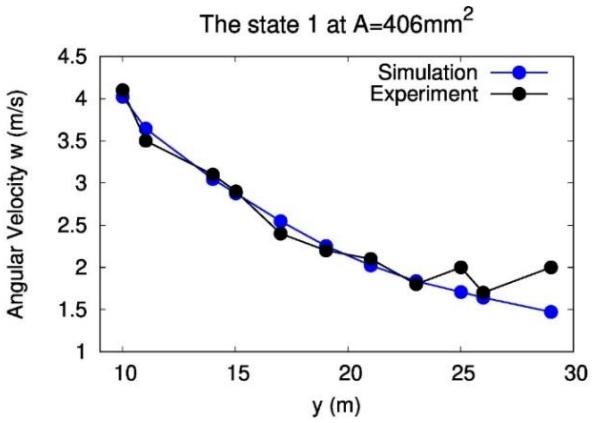

Fig. 14: The angular velocity profile at the inlet for case 1 with 20 gallons/min

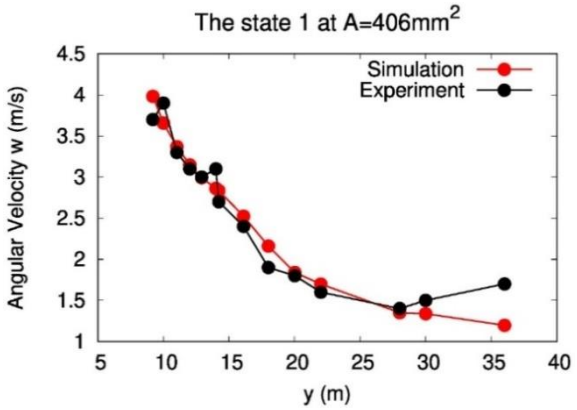

Fig. 15: The angular velocity profile at the outlet for case 1 with 20 gallons/minute

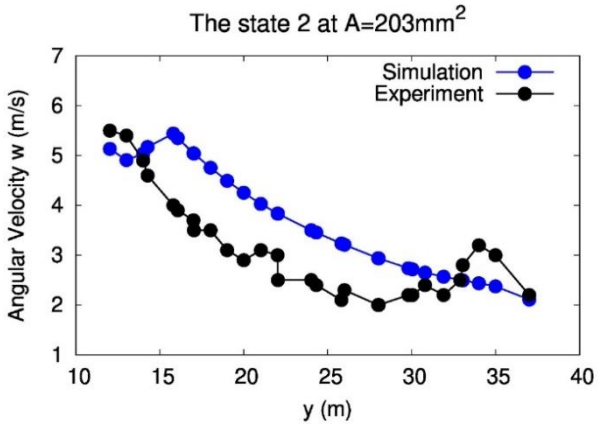

Fig. 16: The angular velocity profile at the outlet for case 2 with 7.5 gallons/min

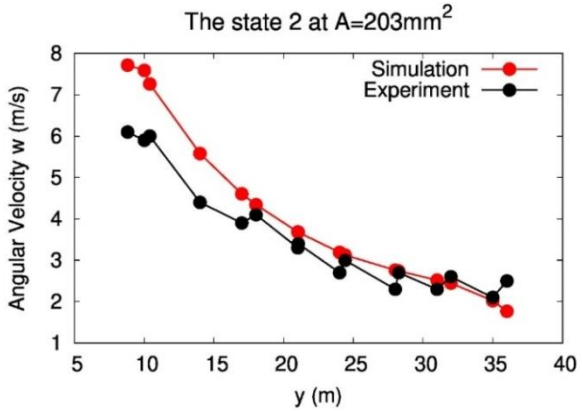

Fig. 17: The angular velocity profile at the outlet for case 2 with 15 gallons/min

From Figures (15) and (16), we observe that the numerical simulation results for case 2 deviate sharply from the experimental results. If we define the average error as:

$$I_{error} = \frac{1}{N}\sum_{i=1}^{i=N}\frac{\sqrt{(x_{i,exact} - x_{i,smulation})^2}}{x_{i,exact}} \qquad (12)$$

Where N is t number of data, $x_{i,exact}$ is the exact value obtained from experiment, and $x_{i,smulation}$ is the data obtained from simulation.

By applying Equation 7, the average errors of 6.11% and 7.18% for case 1 with volume flow rates of 20 gallons per minute at the inlet and outlet were obtained, respectively. For the case 2, we obtained average error of 49.05% and 14.46% with volume flow rate of 15 gallons per minutes at inlet and outlet, respectively. The large error number observed in case 2 could be attributed to the failure of the laminar-flow assumption in that case and underscores the need to implement turbulence modeling or direct numerical simulation for high-Reynolds and high-Weber-number cases.

Flow characteristics of pressure-swirl atomizer

To further assess the performance of the interFoam, we compared the flow characteristics, such as the flow number, spray cone angle, and discharge coefficient obtained from the numerical results with those obtained from the experiment and the literature of the inviscid flow analysis and maximum flow theory explored by Rizk [17] and Benjamin [18]. Moreover, an additional flow rate for each case reported in the experiment was included: 15 gallons per minute for case 1 and 10 gallons per minute for case 2 [14].

Figures (18) show the flow number as a function of the volume flow rate, obtained experimentally, by numerical simulation, and from the literature findings, for cases 1.

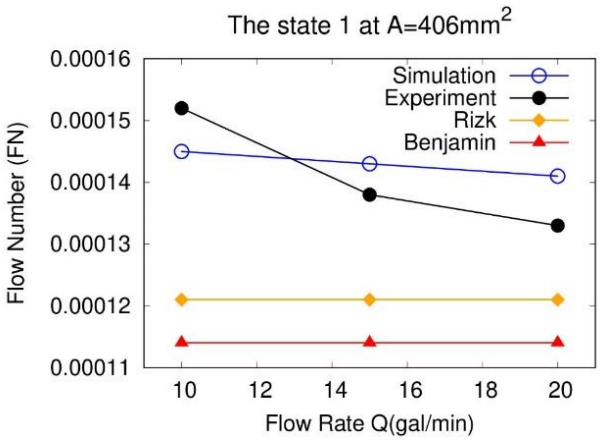

Fig. 18: Flow number obtained by experiment, simulation, and literature for case 1

It is clear from Figure (18) that the numerical simulation is closer to the experimental results than those obtained from the literature.

Figures (19) show the discharge coefficient as a function of the volume flow rate, obtained experimentally, by numerical simulation, and from the literature findings, for case 1.

It can be observed that the discharge coefficient obtained by numerical simulation is closer to the experimental results than those obtained in the literature.

Figure (20) shows the spray cone angle as a function of the volume flow rate, obtained experimentally, by numerical simulation, and from the literature findings, for case 1.

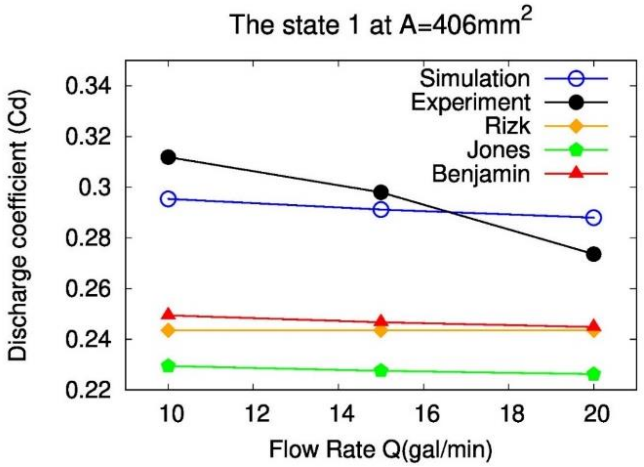

Fig. 19: Discharge coefficient obtained by experiment, simulation, and literature for case 1

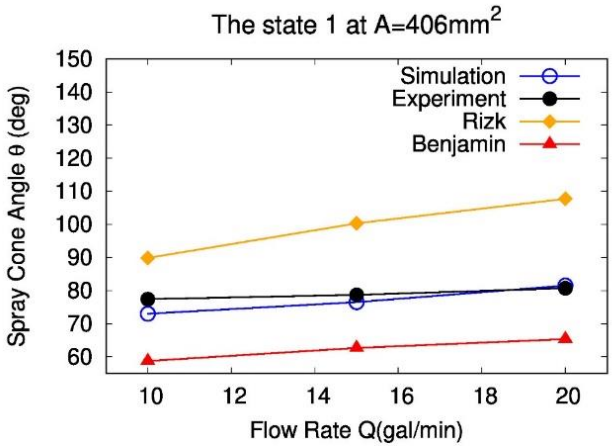

Fig. 20: Spray cone angle obtained by experiment, simulation, and literature for case 1

It can be observed that the spray cone angle obtained by numerical simulation is very close to the experimental results from those obtained from the literature's findings.

Figure (21) shows the flow number as a function of the volume flow rate, obtained experimentally, by numerical simulation, and from the literature findings, for case 2.

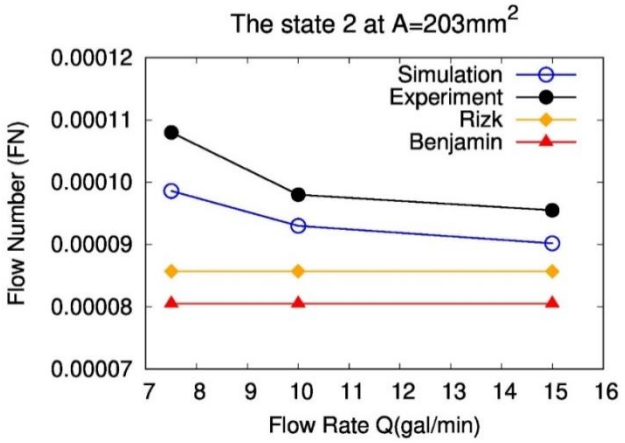

Fig. 21: Flow number obtained by experiment, simulation, and literature for case 2

It can be observed that the discharge coefficient obtained by numerical simulation is closer to the experimental results than those obtained in the literature.

Figure (22) shows the discharge coefficient as a function of the volumetric flow rate, obtained experimentally, from numerical simulations, and from the literature, for case 2.

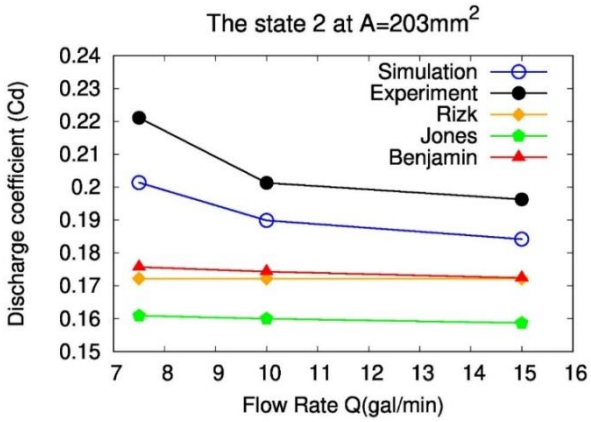

Fig. 22: Discharge coefficient obtained by experiment, simulation, and literature for case 2

It can be observed that the discharge coefficient obtained by numerical simulation is closer to the experimental results than those obtained in the literature.

Figure (23) shows the spray cone angle as a function of the volume flow rate, obtained experimentally, by numerical simulation, and from the literature findings, for case 2.

It can be observed that the results obtained by numerical simulation are comparable to those obtained by the Rizk formula and in better agreement with the experimental results than those obtained by Benjamin and Jones.

It can be clearly noticed that the interFoam solver can represent the flow characteristics, such as the discharge coefficient, flow number, and the spray cone angle, better than the analytical methods that rely on inviscid analysis and maximum flow theory, which indicates the importance of representing the viscous force and shear stress within the flow of a pressure swirl atomizer.

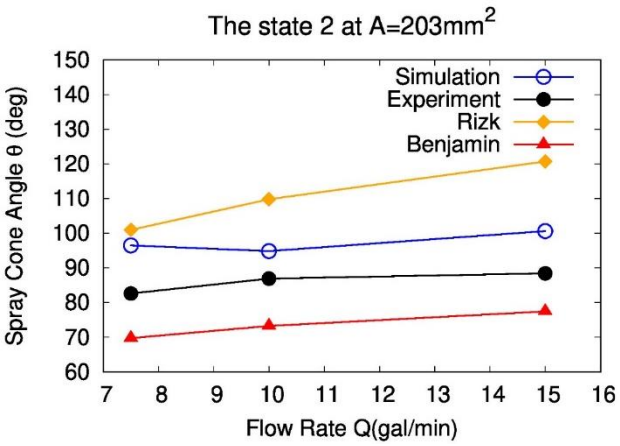

Fig. 23: Spray cone angle obtained by experiment, simulation, and literatures for case 2

Conclusion

In this study, we conducted numerical simulations of a 2D axisymmetric pressure-swirl atomizer using the interFoam solver, considering two distinct cases with different inlet dimensions. InterFoam effectively captured the flow within the pressure-swirl atomizer, where an air core formed and a swirling sheet emanated from the atomizer. Moreover, interFoam qualitatively captures the pressure distribution inside and outside the atomizer. Furthermore, the swirling velocity at the inlet and the exit of the atomizer was analyzed.

We concluded that, for case 1, in which the inlet port area is larger than in case 2, the interFoam results are very close to the experimental data, with an average error of 6.11%. However, the interFoam solver failed to predict reasonable swirling-velocity results at the inter and exit locations of the atomizer, compared with the experimental data for case 2. Furthermore, the deviation from the experimental results was significant, with an average error of 49.05%, underscoring the importance of adopting turbulence models for very high Reynolds numbers to capture near-wall velocity field behavior. Regarding the flow characteristic, namely the flow number, discharge coefficient, and spray cone angle, interFoam provides reasonable results in comparison with those obtained by the analytical solution that relies on inviscid flow analysis and maximum flow theory. The study ignored the effect of swirl number on the flow within the atomizer. Thus, Future studies will investigate the relationship between the swirl number and the transition to turbulence. Moreover, the atomization and breakup modes as a function of the injected pressure will be studied in the future.

Author Contributions: Salem: Conceptualization and methodology, writing—original draft preparation, review and editing**. Aqila and Hamdan**: Data collection, results' analysis and discussion. All authors have read and agreed to the published version of the manuscript.

Funding: "This research received no external funding."

Data Availability Statement: "No data were used to support this study."

Conflicts of Interest: "The authors declare that they have no conflict of interest.

REFRENCES

[1] G. Vijay, et al. "Internal and external flow characteristics of swirl atomizers: A review". *Atomization and Sprays*, vol. 25, no. 2, 2015, pp. 153–188. https://doi.org/10.1615/Atomiz5pr. 2014010219.

[2] B. Sumer, et al. "Experimental and Numerical Investigation of a Pressure Swirl Atomizer". *ICLASS 2012, 12th Triennial International Conference on Liquid Atomization and Spray Systems*, Heidelberg, Germany, 2012.

[3] C. Galbiati, S. Tonini, P. Conti, and G. Cossali. "Numerical Simulations of Internal Flow in an Aircraft Engine Pressure Swirl Atomizer." *Journal of Propulsion and Power*, vol. 32, no. 6, pp. 1433–1441, 2016. https://doi.org/10.2514/1.B36015.

[4] Z. Liu, et al. "Studies on air core size in a simplex pressure-swirl atomizer". *International Journal of Hydrogen Energy*, vol. 42, no. 29, 2017, pp. 18649–18657. https://doi.org/10.1016/j.ijhydene.2017.04.188.

[5] J. Ronceros, et al. "Study of Internal Flow in Open-End and Closed Pressure-Swirl Atomizers with Variation of Geometrical Parameters". *Aerospace*, vol. 10, no. 11, 2023, pp. 930. https://doi.org/10.3390/aerospace10110930.

[6] M. Malý, et al. "2D and 3D numerical modelling of internal flow of Pressure-swirl atomizer". *EPJ Web of Conferences*, vol. 213, 2019, pp. 02055. https://doi.org/10.1051/epjconf/201921302055.

[7] A. Nouri-Borujerdi, et al. "Numerical Simulation of Laminar and Turbulent Two-Phase Flow in Pressure-Swirl Atomizers". *AIAA Journal*, vol. 50, no. 10, 2012, pp. 2091–2101. https://doi.org/10.2514/1.J051331.

[8] O. Baran, et al. "Experimental and Numerical Investigation of Coaxial Pressure Swirl Injectors". *AIAA SciTech Forum*, San Diego, California, 2019, pp. AIAA 2019-1740. https://doi.org/10.2514/6.2019-1740.. AIAA SciTech Forum, San Diego, California. AIAA 2019-1740. doi: 10.2514/6.2019-1740.

[9] C. W. Hirt, et al. "Volume of Fluid (VOF) Method for the Dynamics of Free Boundaries". *Journal of Computational Physics*, vol. 39, no. 1, 1981, pp. 201–225. https://doi.org/10.1016/0021-9991(81)90145-5.

[10] C. W. Hirt, et al. "Volume of Fluid (VOF) Method for the Dynamics of Free Boundaries". *Journal of Computational Physics*, vol. 39, no. 1, 1981, pp. 201–225. https://doi.org/10.1016/0021-9991(81)90145-5.

[11] S. S. Deshpande, et al. "Evaluating the performance of the two-phase flow solver interFoam". *Computational Science & Discovery*, vol. 5, no. 1, 2013, pp. 014016. https://doi.org/10.1088/1749-4699/5/1/014016.

[12] D. Ferrando, et al. "Modeling internal flow and primary atomization in a simplex pressure-swirl atomizer". *Atomization and Sprays*, vol. 33, no. 3, 2023, pp. 1–28. https://doi.org/10.1615/AtomizSpr.2022045618

[13] A. Salem, et al. "The Potential of the Simple Coupled Volume of Fluid and Level Set Method in OpenFOAM to Elucidate the Flow of Pressure Swirl Atomizer". *Proceedings of the International Conference for Mechanical and Industrial Engineering (ICMIE)*, 2023. https://doi.org/10.13140/RG.2.2.14666.85448.

[14] Z. Ma, et al. "Investigation on the Internal Flow Characteristics of Pressure-swirl Atomizer". *Doctoral dissertation, University of Cincinnati*, 2001.

[15] K. Xie, et al. "Numerical simulation of the flow characteristics within a pressure-swirling atomizer". *Proceedings of ASME Turbo Expo 2014: Turbine Technical Conference and Exposition*, Düsseldorf, Germany, 2014, pp. GT2014-26788. https://doi.org/10.1115/GT2014-26788.

[16] K. Khani Aminjan, et al. "Experimental and numerical study on inlet pressure and Reynolds number in tangential input pressure-swirl atomizer". *Arabian Journal for Science and Engineering*, 2025. https://doi.org/10.1007/s13369-024-09923-5.

[17] N. K. Rizk, et al. "Prediction of velocity coefficient and spray cone angle for simplex swirl atomizers". *International Journal of Turbo and Jet-Engines*, vol. 4, no. 1-2, 1987, pp. 65–73. https://doi.org/10.1515/tjj.1987.4.1-2.65.M.

[18] M. A. Benjamin, et al. "Spray characterization of a relatively high flow simplex atomizer using experiment and CFD". *32nd Joint Propulsion Conference and Exhibit*, Lake Buena Vista, FL, 1996, pp. AIAA 1996-3165. https://doi.org/10.2514/6.1996-3165.

[19] J. Jeon, et al. "Experimental study on spray characteristics of gas-centered swirl coaxial injectors". *Journal of Fluids Engineering*, vol. 133, no. 12, 2011, pp. 121303. https://doi.org/10.1115/1.4005344.

[20] M. A. Uzun, et al. "Formation of Görtler vortices in an open-end pressure swirl atomizer". *Physics of Fluids*, vol. 37, no. 4, 2025, pp. 043320. https://doi.org/10.1063/5.0253204.

[21] A. Han, et al. "Numerical study and validation of the near-nozzle spray behavior of a non-proprietary pressure-swirl atomizer for aviation applications". *ASME Turbo Expo 2025: Turbomachinery Technical Conference and Exposition*, vol. 88780, 2025, pp. V03AT04A057. https://doi.org/10.1115/GT2025-141872.

[22] O. Ubbink, et al. "Numerical prediction of two fluid systems with sharp interfaces". *Ph.D. Thesis, Imperial College of Science, Technology and Medicine*, London, 1997.